JOURNAL OF COMPUTATIONAL BIOLOGY
Volume 22, Number 3, 2015

Pp. 227–235
DOI: 10.1089/cmb.2014.0198

An Approximative Approach for Single Cell Spatial Modeling of Quorum Sensing

MELTEM GÖLGELI MATUR,[1] JOHANNES MÜLLER,[1,2] CHRISTINA KUTTLER,[1,2] and BURKHARD A. HENSE[1]

ABSTRACT

Quorum sensing, a special kind of cell–cell communication, has originally been described for well-mixed homogeneous bacterial cultures. However, recent perception supports its ecological relevance for spatially heterogeneous distributed cells, like colonies and biofilms. New experimental techniques allow for single cell analysis under these conditions, which is crucial to understanding the effect of chemical gradients and intercell variations. Based on a reaction-diffusion system, we develop a method that drastically reduces the computational complexity of the model. In comparison to similar former approaches, handling and scaling is much easier. Via a suitable scaling, this approach leads to approximative algebraic equations for the stationary case. This approach can be easily used for numerical situations.

Key words: algorithms, computational molecular biology, evolution.

1. INTRODUCTION

WE MORE AND MORE UNDERSTAND THAT bacteria are not isolated individuals, but that having interaction is central for them to perform well in different environments. Communication is one method to optimize their behavior. Experiments target on the investigation of these communication structures. It is technically more and more possible to address the behavior of single cells. Classical reaction-diffusion models rather formulate dynamics on the level of population densities. These models have only a limited use with respect to high-resolution experiments. However, they have the advantage that many mathematical techniques are available to analyze these models (Logan, 2008).

On the other extreme, sophisticated stochastic simulation models are used to predict the behavior of single cells. These models may be realistic, but are nontreatable anymore (Alpkvist et al., 2001; Czárán and Hoekstra, 2009). We aim at a simple, deterministic, spatially structured approach that allows formulation of the state of single cells and is still analytically treatable. The considerations here are closely related to modeling approaches formulated in Müller and Uecker (2012); Müller et al. (2006); and Uecker et al. (2014). The difference is that in these models, cells are balls that control in- and outflow. That is, the signaling substance must not passively diffuse through the cell wall. However, this is the case for most small signaling substances as many acyl homoserine lactones (AHLs) (Kaplan & Greenberg, 1985). Bacterial cell–cell communication, usually called quorum sensing, has been described as a mechanism to

[1]Institute of Computational Biology, Helmholtz Zentrum München, Neuherberg, Germany.
[2]Centre of Mathematical Sciences, Technische Universität München, Garching, Germany.

ensure coordinated behavior on population level. In short, cells release signaling substances and measure the environmental concentration of it. In response to this concentration, expression of genes, usually involved in cooperative behavior, are regulated. As most pathogens regulate their virulence by quorum sensing systems, this control strategy is of high human interest. A positive feedback loop, which is included in most known quorum sensing systems, that is, upregulation of the signal production, was suggested to allow for an all-or-none reaction of the population. Thus, two states can be distinguished: a noninduced state with low signal production and an induced state with higher production.

In this context, quorum sensing has usually been analyzed on population level, both experimentally and in modeling. Whereas this may often be adequate for mixed planktonic scenarios, most bacteria rather live spatially fixed, for example, on surfaces as single cells, microcolonies, or biofilms. Under such spatially heterogeneous conditions, gradients of, for example, signal concentrations can emerge. Thus, high-resolution analysis is essential (Carnes et al., 2010; Hense et al., 2007; Meyer et al., 2012).

In the present work, we address exactly this situation of single cells in the stationary case, but omit the cell walls. Cells are defined as places in space where signaling substance is produced. One advantage is that the number of parameters is reduced: only the diffusion constant is required, no transport mechanism through the cell wall needs to be defined. We simplify the model in the same spirit as in Müller and Uecker (2012), Müller et al. (2006), and Uecker et al. (2014), and can thereby replace the original problem by a point source problem. However, also in this point the setting we consider here has an advantage: the approximation theorems are considerably more simple.

We apply the resulting, rather simple, model equations to observations for *Pseudomonas putida*, for example, to investigate the influence of the diffusion rate and the spatial arrangement of the bacteria on the communication. We will exemplarily apply our resulting model to look at several biological questions. Whereas most experiments are conducted in aqueous culture media, the diffusion properties of the matrix in natural situations may vary. Bacteria are found in the mucus on gut or lung epithel. Here, the diffusion rates are lower, especially in, for example, patients with cystic fibrosis (Matsui et al., 2006). The question arises whether this difference could affect the basics of cell–cell communication. We will thus simulate such a scenario for different spatial cell arrangements.

2. MODEL

We consider N ball-shaped cells located in $x_1, \ldots, x_N \in \mathbb{R}^3$ with radius R. Cell i occupies $\Omega_i = \{|x - x_i| < R\}$. Let $u(x, t)$ denote the concentration of signaling molecules, and

$$\overline{u}_i(t) = \frac{1}{R^3\omega}\int_{\Omega_i} u(x,t)dx$$

the concentration averaged over a ball of radius R (the location of the cells). We assume that the regulatory network of cells sense this average concentration, and produce at rate $f(\overline{u})$ signaling substance. For the time being, we assume that f is differentiable, bounded, strictly monotonously increasing, and $f(0) > 0$. The produced signaling substance diffuses at rate D and is degraded at rate γ. Taken together, we obtain the reaction-diffusion equation

$$u_t = D\Delta u - \gamma u + \sum_{i=1}^{N} \chi_{\Omega_i}(x) R^{-3} f(R^1 \overline{u}_i). \tag{1}$$

The heuristics for the scaling introduced in this equation is the following: A cell of radius R will produce signaling substance at a rate proportional to its size, that is, proportional to R^3; the factor $R^{-3}f(\cdot)$ balances this effect. In order to understand the scaling of the argument of $f(\cdot)$, we note that a cell is expected to resemble a point source for small R. The concentration develops a pole of first order, and hence also the average $\overline{u}_i$ will blow up with $1/R$. The scaling $R\overline{u}_i$ of the argument ensures that it is of order $\mathcal{O}(R^0)$. These considerations only reflect the rationale for the scaling. The computations below show that this scaling is sensible indeed. We aim at an approximative L^2-solution of the stationary state, denoted by v. As a technical trick, we artificially tag the molecules of the signaling substance by the cell that produced the molecule see Fig. 1 for a sketch). Let $v_i(x, t)$ denote the concentration of signaling substance produced by cell i, then $v(x, t) = \sum v_i(x, t)$. Furthermore, we introduce

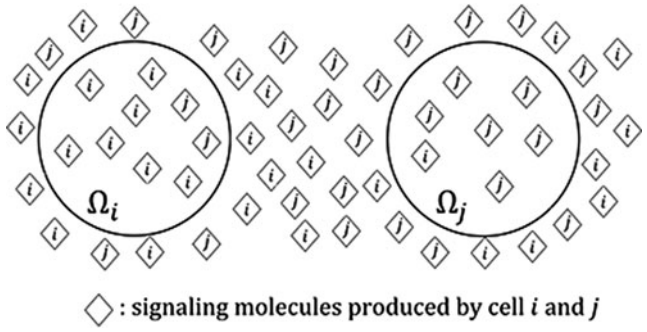

FIG. 1. Signaling molecule production of each cell and diffusion in and out of

$$\overline{v}_{i,j} = \frac{1}{R^3\omega}\int_{\Omega_j} v_i(x,t)dx,$$

the average of the signaling molecules produced by cell i in the inner of cell j. This is assumed to govern the reaction term. The reaction-diffusion equation (1) expands into a system of reaction-diffusion equations

$$(v_i)_t = Dr\Delta v_i - \gamma v_i + \chi_{\Omega_i}(x)R^{-3}f(R^1\sum_{j=1}^{N}\overline{v}_{j,i}) \tag{2}$$

A short computation shows that, given v_i, the function $u = \sum v_i$ indeed solved (1). Vice versa, if we have a solution u, the linear, inhomogeneous equation

$$(v_i)_t = D\Delta v_i - \gamma v_i + \chi_{\Omega_i}(x)R^{-3}f(R^1\overline{u}_i) \tag{3}$$

defined functions v_i that in turn satisfy (2).

3. ONE CELL

In case of one cell, (1) and (2) coincide. The stationary solution in this case can be analytically reduced to a fixed point equation. Without restriction, we assume that the cell is located in $x_1 = 0 \in \mathbb{R}^3$. Since the substance production is only possible within the cell, the outer substance concentration is comprised by free diffusion through the cell wall. In this case, we expect a radially symmetric solution. In polar coordinates, (2) reads (for $N = 1$)

$$0 = \frac{d^2}{dr^2}v(r) + \frac{2}{r}\frac{d}{dr}v(r) - \gamma/Dv(r) + \chi_{r<R}m/D \tag{4}$$

with $m = R^{-3}f(R^1\overline{v}_1)$ and $v(r)$ bounded, $v(r) \to 0$ for $r \to \infty$. Obviously, we distinguish between the intracellular and the extracellular space.

Proposition 1 *The solution for Equation (4) in terms of m reads for $r < R$*

$$v(r) = \frac{m}{\gamma}\left[1 + \left(R + \sqrt{\frac{D}{\gamma}}\right)\frac{\sinh\left(-\sqrt{\gamma/D}r\right)}{r}e^{-\sqrt{\gamma/D}R}\right] \tag{5}$$

and for $r > R$

$$v(r) = m\ \eta(R)\frac{e^{-\sqrt{\gamma/D}r}}{r} \tag{6}$$

with

$$\eta(R) = \frac{1}{\gamma}\left[R\cosh\left(\sqrt{\gamma/D}R\right) + \sqrt{D/\gamma}\sinh\left(-\sqrt{\gamma/D}R\right)\right] = R^3/(3D) + \mathcal{O}(R^4).$$

For the proof see Appendix A.

We now compute $\overline{u}_1$.

Proposition 2

$$\overline{u}_1 = \frac{1}{R^3\omega}\int_{r<R} u(r)4\pi r^2\ dr = m\ \theta(R) \tag{7}$$

with

$$\begin{aligned}\theta(R) &= \frac{1}{\gamma}\left[1+3\frac{D}{\gamma}\left(R+\sqrt{\frac{D}{\gamma}}\right)\times\frac{(\sinh(\sqrt{\gamma/D}\ R)-\sqrt{\gamma/D}\ R\cosh(\sqrt{\gamma/D}\ R))}{R^3}e^{-\sqrt{\gamma/D}\,R}\right]\\ &= \frac{2}{5D}R^2-\frac{1}{3D}\sqrt{\frac{\gamma}{D}}R^3+\mathcal{O}(R^4)\end{aligned} \tag{8}$$

Proof: Use $(\sinh(x) - x\cosh(x))' = x\sinh(x)$. ■

The computation of a stationary point is equivalent to a fixed point equation,

$$m = R^{-3}f(R^1\overline{u}_1) = R^{-3}f(\theta(R)\ R^1\ m). \tag{9}$$

Recall the properties of $f(\cdot)$: f is differentiable, bounded, strictly monotonously increasing, and $f(0) > 0$. Thus, we find at least one solution $\hat{m}$. This solution depends on R.

Theorem 3 *For $N = 1$, Equation (1) possesses at least one positive, radial symmetric, stationary solution in $L^2(\mathbb{R}^3)$.*

We aim to investigate the outer solution $u(r)$, $r > R$, for small R, in particular in the limit $R \to 0$, again by using approximative solutions.

Theorem 4 *Consider one cell only, $N = 1$. Let $u_R(r)$ be a family of solutions of Equation (1) for $R > 0$, which is smooth in R. Then, there is a solution $v(r)$ (and M_0) of*

$$0 = D\Delta v - \gamma v + \frac{4\pi M}{3D}\delta_0 \tag{10}$$

$$M = f(2M/(5D)) \tag{11}$$

such that

$$\|u_R(r) - v(r)\|_{L^2(\{|x|>R\})} \le CR.$$

if R is small enough. Furthermore,

$$|R\overline{u}_R - M| = \mathcal{O}(R).$$

Proof: The nonlinear problem can be solved if we know $m = R^{-3}f(R^1\overline{v}_1)$. We find a fixed point Equation (9) for m. If we define $M = mR^3$, this equation becomes $M = f(\theta(R)R^{-2}M)$. As $\theta(R)R^{-2} \to 2/(5D)$ for $R \to 0$, we obtain a smooth family of solutions $M = M(R)$, where $M(R)$ converges to a solution M_0 of (11).

For $r > R$ we find the outer solution given by

$$u_R(r) = M(R)R^{-3}\eta(R)\frac{e^{-\sqrt{\gamma/D}r}}{r} \to \frac{M_0}{3D}\frac{e^{-\sqrt{\gamma/D}r}}{r} = v(r) \tag{12}$$

where the limit is pointwise; $v(r)$ satisfies (10). We find

$$\begin{aligned}\|u_R - v\|^2_{L_2(\{|x|>R\})} &= \int_R^\infty 4\pi r^2(u_R(r)-v(r))^2 dr\\ &= \left(M(R)R^{-3}\eta(R) - \frac{M_0}{3D}\right)^2\int_R^\infty 4\pi\ \left(e^{-\sqrt{\gamma/D}\,r}\right)^2 dr\\ &= \mathcal{O}(R^2).\end{aligned}$$

This estimate establishes the L^2 convergence on $\{|x| > R\}$. The estimate $|R\overline{u}_R - M| = \mathcal{O}(R)$ is a direct consequence of the definition of M and Prop. 2. ■

Remark 5 Basically we find that—for R small—we are allowed to replace our original model (1) by a point source (10) and (11): The outer solution (concentration of signaling substance) can be approximated as well as the mean concentration $\overline{u}_R$, which triggers the response of a cell.

4. N CELLS

We now turn to the case of N cells of radius R, located in $x_1, \ldots, x_N$. The aim is to prove also in this case a theorem similar to Theorem 4. Therefore, we replace in (2) the term $R^{-3}f(R^1 \sum_{j=1}^{N} \overline{v}_{j,i})$ by given constants m_i. In this case, the equations decouple, and we are back again in the case for one cell. The solution is given by (5) and (6). This explicit solution allows to compute $\overline{v}_{i,j}$ explicitly in the leading orders in R. We already know

$$\overline{v}_{i,i} = m_i \theta(R) = \frac{2m_i}{5D} R^2 - \frac{m_i}{3D} \sqrt{\frac{\gamma}{D}} R^3 + \mathcal{O}(R^4)$$

and for $i \neq j$

$$\overline{v}_{i,j} = m_j \, \eta(R) \left(\frac{e^{-\sqrt{\gamma/D}\|x_i - x_j\|}}{\|x_i - x_j\|} + \mathcal{O}(R) \right) = \frac{m_j}{3D} \frac{e^{-\sqrt{\gamma/D}\|x_i - x_j\|}}{\|x_i - x_j\|} R^3 + \mathcal{O}(R^4).$$

If we introduce as before $M_i = R^3 m_i$, the consistency condition reads

$$M_i = f\left(\frac{2M_i}{5D} - \frac{M_i}{3D} \sqrt{\frac{\gamma}{D}} R + \sum_{i \neq j} \frac{e^{-\sqrt{\gamma/D}\|x_i - x_j\|} M_j}{3D\|x_i - x_j\|} R + \mathcal{O}(R^2) \right). \tag{13}$$

We obtain an approximation theorem for the solutions v_i of (3).

Theorem 6 *Assume that there is a hyperbolic solution of*

$$\tilde{M}_i = f\left(\frac{2\tilde{M}_i(R)}{5D} - \frac{\tilde{M}_i \, R}{3D} \sqrt{\frac{\gamma}{D}} + \sum_{i \neq j} \frac{e^{-\sqrt{\gamma/D}\|x_i - x_j\|} \tilde{M}_j R}{3D\|x_i - x_j\|} \right). \tag{14}$$

Let furthermore $\tilde{v}_i \in L^2$ the functions that satisfy

$$0 = D\Delta \tilde{v}_{i,R} - \gamma \tilde{v}_{i,R} + \frac{4\pi \tilde{M}_i}{3D} \delta_{x_i}.$$

Then, there is a solution $v_{i,R}(r)$ of (3) that is in $L^2(\{|x - x_i| > R)\}\mathcal{O}(R)$-close to $v_{i,R}$, such that

$$\|v_{i,R}(r) - \tilde{v}_{i,R}(r)\|_{L^2(\{|x - x_i| > R\})} \leq CR. \tag{15}$$

if R is small enough. Furthermore,

$$|R\overline{v}_{R,i,i} - \tilde{M}_i| = \mathcal{O}(R^2). \tag{16}$$

Proof: As the solution of (14) is hyperbolic, we may perturb this system weakly, and still find a solution close by. To be more precise, if R is sufficiently small, we find solutions M_i of (13) s.t.

$$|M_i - \tilde{M}_i| = \mathcal{O}(R^2).$$

This observation establishes (16). The inequality (15) follows in a similar way as in the one-cell-case (see proof of Theorem 4). ■

Table 1. Chosen Standard Parameter Values for the Simulations for *P. putida* with the Signaling Substance AHL

Parameter	*Description*	*Value*	*Reference*
α	AHL production rate	2.3×10^3 $[\frac{nmol}{l\cdot h}]$	a
β	induced AHL production rate	2.3×10^4 $[\frac{mol}{l\cdot h}]$	a
D	diffusion rate in water	3232542 $[\frac{\mu m^2}{h}]$	b
D	diffusion rate in 2.5% mucus	1728000 $[\frac{\mu m^2}{h}]$	c
D	diffusion rate in 8% mucus	176400 $[\frac{\mu m^2}{h}]$	c
A_{thresh}	induction threshold of AHL	70 $[\frac{nmol}{l}]$	a
γ	degradation rate of AHL	0.005545/h	d

[a]According to Fekete et al. (2010).
[b]Diffusion rate in water according to Hobbie (1988).
[c]Diffusion rates in mucus according to Matsui et al. (2006).
[d]According to Englmann et al. (2007).

5. APPLICATION

Next, we used the approximative system as introduced above to simulate some typical situations. All simulations are shown for bacteria distributed randomly on a square-shaped area of side lengths 300 μm. For the chosen parameter values, see Table 1. As concrete production term for the signaling substance (i.e., production and degradation), we choose

$$f(u)=\alpha+\beta\frac{u}{A_{thresh}+u}$$

This corresponds to a simplified version of the positive feedback loop for *P. putida*, with Hill coefficient $n = 1$ (see Fekete et al., 2010).

We start with the situation of two cells of *P. putida* with the distance of approximately 100 μm from each other, under different diffusibility conditions, (see Fig. 2). The left picture shows bacteria in an aqueous environment; the central picture in an environment of reduced diffusibility (0.1 of the value in water), as for example in a kind of biofilm; the right picture in an environment of even more reduced diffusibility (0.01 of the value in water). Obviously, there is no difference in the qualitative behavior, but the peak concentration differs: as expected, in a situation with less diffusion, the signaling substance can accumulate better, leading to higher concentrations in the peaks (see the scale). Please note that a logarithmic scale has been used for the signaling substance concentration in the plots, due to better visibility and comparability.

Of course, our method also allows for computing the signaling substance distribution in real world problems. Exemplarily, we show a situation for the pathogenic bacteria species *Pseudomonas aeruginosa* in (spatially unlimited) lung mucus in Figure 3. These bacteria may be very harmful, especially for patients with cystic fibrosis (CF), who have a more viscous mucus compared to healthy people. The signaling substance parameters are assumed to be similar to those of *P. putida*, but with pH 7.3, which influences the degradation of the signaling substance (Englmann et al., 2007). Furthermore, we can compare different viscosity situations, concerning the diffusibility, to the situation in water. Obviously, in mucus stronger accumulation takes place, leading to an easier induction of the system. The activation threshold is 70 nmol/l

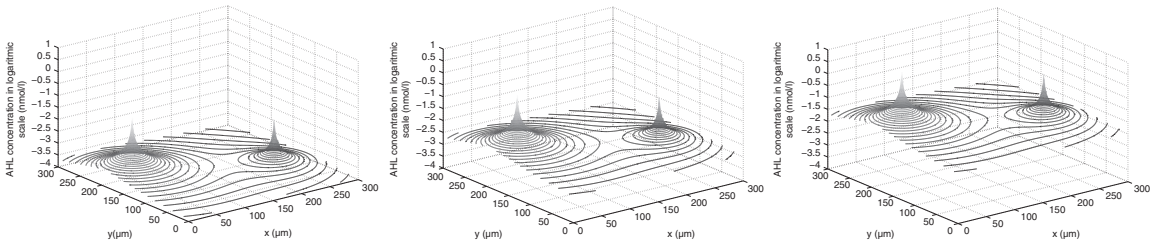

FIG. 2. Situation of two cells, with different diffusion rates: water (left), 0.1 times that of water (center), and 0.01 times that of water (right)

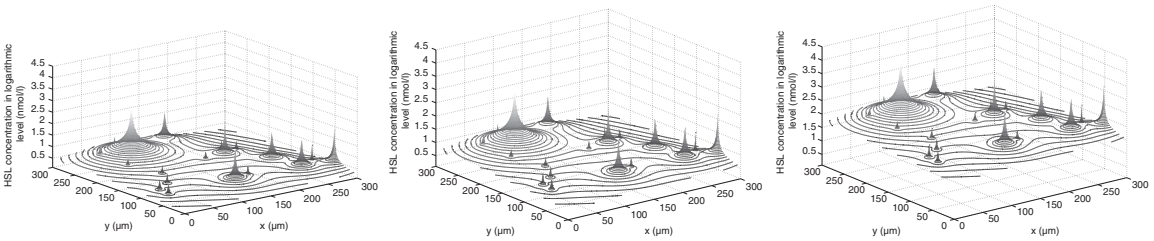

FIG. 3. Situation of 20 cells randomly distributed in space, adapted to the situation in lung mucus: water (left), 2.5% mucus (center), and 8% mucus (right).

(Table 1), which corresponds to approximately 1.8 in the logarithmic scale in Figure 3, where 20 randomly distributed cells are shown. There, one fines several bacteria, which are not activated in the situation in water, but in the corresponding mucus situation. By that, the bacteria may become more and aggressive earlier than in ''normal'' patients.

6. DISCUSSION

By the approach presented here, we get a simpler possibility to understand the necessary scaling for the approximative solution as, for example, in Müller and Uecker (2012); Müller et al. (2006); and Uecker et al. (2014). As a result, we get a handy method for the numerical solution of stationary signaling substance distributions for single cells located in $\mathbb{R}^3$. By using ''mirror cells'' (as usual, e.g., in electrostatics), many confined geometries as half-spaces and cubes can be handled. Of course, it is not realistic to deal with unlimited space, but as the diffusion of the signaling substance does not reach very far, this doesn't play a major role for practical purposes.

One relevant restriction concerns the distance between the single cells: The approximation is only valid if the distance between cells is large in comparison with their diameter. Nevertheless, colonies with many close cells can be easily simulated when handling the complete colony like one cell, where the production rate is upscaled accordingly.

The simulations indicate that significant concentration gradients may emerge on microscale in a spatially structured environment. It turns out that these gradients are of special importance for situations with low diffusion rates, as can be found in, for example, mucus of some host epithelia or in the EPS matrix of biofilms. The quorum sensing system is affected in two different ways: First, signal concentrations close to the cells are higher. Therefore, smaller colonies are sufficient to induce the system. In fact, under extreme diffusion confined conditions even a single cell may be sufficient for induction (Carnes et al., 2010). Second, the relative influence of neighboring cells or colonies for induction decreases compared to the relevance of the cell itself or the colony in which it grows. In other words, communication becomes more ''private''. This reminds of the results of Fujimoto and Sawai (2013), who reported that reduced transport of signals through the cell membrane results in a rather autonomous cell decision, whereas fast export supports a common of the group. In other words, with low diffusion rates the influence of other cells or colonies decreases, that is, the communication aspect of quorum sensing declines. All in all, communication is broken if the diffusion coefficient is small. In this case, we cannot expect a synchronized, homogeneous response of the complete population. The simulations indicate that in this case the population fragments are in small, heterogeneous subpopulations. Similar to the results of Fujimoto and Sawai (2013), on population level, this could principally change an all-or-nothing decision during growth into a rather graded decision, although on single cell level the upregulation will remain switchlike. Changes of globality versus privacy in communication have an impact on possible treatment strategies that aim at interfering with extracellular signaling.

Our results enable first insights into the fascinating question about the relevance of microscale communication. It is connected with aspects of stability against cheaters, that is, mutants that do not contribute to, but benefit from, the cooperation (Hense et al., 2007). Furthermore, the purpose of intra- or extracellular signal degrading enzymes produced by the signaling cells themselves may be only fully understood if investigated in microscale. As this resolution is still difficult to approach experimentally, mathematical modeling and simulations provide central tools that allow for analyzing these effects.

APPENDIX A: COMPUTATIONS FOR PROP. 1

In order to solve Equation (4), we use the transformation

$$v(r) = s(r)/r, \qquad s(0) = 0$$

and find

$$0 = s'' - \gamma/Ds + r\chi_{r<R}m/D. \tag{17}$$

The solution is the sum of the homogeneous and the inhomogeneous solution. For the homogeneous solution of (17), we obtain

$$s(t) = Ae^{\sqrt{\gamma/D}r} + Be^{-\sqrt{\gamma/D}r}$$

and the general solution for $r < R$ reads

$$s(t) = Ae^{\sqrt{\gamma/D}r} + Be^{-\sqrt{\gamma/D}r} + \frac{m}{\gamma}r.$$

Hence $s(0) = 0$ implies $B = -A$. Similarly for $r > R$ we have

$$s(t) = \hat{A}e^{\sqrt{\gamma/D}r} + \hat{B}e^{-\sqrt{\gamma/D}r}.$$

Since $s(r)/r \to 0$ for $r \to \infty$, $\hat{A} = 0$, one gets

$$s(t) = \hat{B}e^{-\sqrt{\gamma/D}r}.$$

We require $s(t) \in C^1$. The necessity of the smoothness on the boundary imposes the boundary conditions where the solutions for $r < R$ and $r > R$ have to be equivalent at $r = R$, as well as the first derivatives thereof:

$$A\left(e^{\sqrt{\gamma/D}R} - e^{-\sqrt{\gamma/D}R}\right) + \frac{m}{\gamma}R = \hat{B}e^{-\sqrt{\gamma/D}R}$$

$$A\sqrt{\gamma/D}\left(e^{\sqrt{\gamma/D}R} + e^{-\sqrt{\gamma/D}R}\right) + \frac{m}{\gamma} = -\sqrt{\gamma/D}\hat{B}e^{-\sqrt{\gamma/D}\,R}.$$

Hence,

$$A = -\frac{m}{2\gamma}\left(R + \sqrt{\frac{D}{\gamma}}\right)e^{-\sqrt{\gamma/D}R}$$

and

$$\hat{B} = \frac{m}{2\gamma}\left[\left(R + \sqrt{\frac{D}{\gamma}}\right)e^{-\sqrt{\gamma/D}R} + \left(R - \sqrt{\frac{D}{\gamma}}\right)e^{\sqrt{\gamma/D}R}\right].$$

After computing the coefficients we obtain the explicit solution for $r < R$,

$$s(t) = Ae^{\sqrt{\gamma/D}r} + Be^{-\sqrt{\gamma/D}r} + \frac{m}{\gamma}r.$$

Using $A = -B$ and the value of A derived above, we obtain the explicit solution

$$= \frac{m}{\gamma}\left(R + \sqrt{\frac{D}{\gamma}}\right)\frac{1}{2}\left(e^{-\sqrt{\gamma/D}r} - e^{\sqrt{\gamma/D}r}\right)e^{-\sqrt{\gamma/D}R} + \frac{m}{\gamma}r$$

and

$$u(r) = \frac{m}{\gamma}\left[1 + \left(R + \sqrt{\frac{D}{\gamma}}\right)\frac{\sinh\left(-\sqrt{\gamma/D}r\right)}{r}e^{-\sqrt{\gamma/D}\,R}\right].$$

Respectively, for $r > R$ we get

$$s(r) = \frac{m}{2\gamma}\left[\left(R + \sqrt{\frac{D}{\gamma}}\right)e^{-\sqrt{\gamma/D}\,R} + \left(R - \sqrt{\frac{D}{\gamma}}\right)e^{\sqrt{\gamma/D}\,R}\right]e^{-\sqrt{\gamma/D}\,r}$$
$$= \frac{m}{\gamma}\left[R\cosh\left(\sqrt{\gamma/D}\,R\right) + \sqrt{\gamma/D}\sinh\left(-\sqrt{\gamma/D}\,R\right)\right]e^{-\sqrt{\gamma/D}\,r}$$

and

$$u(r) = \frac{m}{\gamma}\left[R\cosh\left(\sqrt{\gamma/D}\,R\right) + \sqrt{\gamma/D}\sinh\left(-\sqrt{\gamma/D}\,R\right)\right]\frac{e^{-\sqrt{\gamma/D}\,r}}{r}.$$

AUTHOR DISCLOSURE STATEMENT

No competing financial interests exist.

REFERENCES

Alpkvist, E., Picioreanu, C., van Loosdrecht, M., and Heyden, A. 2001. Three-dimensional biofilm model with individual cells and continuum EPS matrix. *Biotech. and Bioeng.* 94, 961–979.

Carnes, E., Lopez, D., Donegan, N., et al. 2010. Confinement-induced quorum sensing of individual *Staphylococcus aureus* bacteria. *Nature Chemical Biology* 6, 41–45.

Czárán, T., and Hoekstra, R. 2009. Microbial communication, cooperation and cheating: Quorum sensing drives the evolution of cooperation in bacteria. *PLoS ONE* 4, e6655, 1–9.

Englmann, M., Fekete, A., Kuttler, C., et al. 2007. The hydrolysis of unsubstituted n-acylhomoserine lactones to their homoserine metabolites; analytical approaches using ultra performance liquid chromatography. *J. Chromotogr.* 1160, 184–193.

Fekete, A., Kuttler, C., Rothballer, M., et al. (2010). Dynamic regulation of n-acyl-homoserine lactone production and degradation in pseudomonas putida isof. *FEMS Microb. Ecol.* 62, 22–34.

Fujimoto, K., and Sawai, S. 2013. A design principle of group level decision making in cell populations. *PLoS Comp. Biol.* 9, e1003110.

Hense, B., Kuttler, C., Müller, J., et al. 2007. Does efficiency sensing unify diffusion and quorum sensing *Nat. Rev. Microbiol.* 5, 230–239.

Hobbie, R. 1988. *Intermediate Physics for Medicine and Biology.* Wiley, London.

Kaplan, H., and Greenberg, E. 1985. Diffusion of autoinducer is involved in regulation of the *Vibrio fischeri* luminescence system. *J. Bacteriol.* 163, 1210–1214.

Logan, J. 2008. *An Introduction to Nonlinear Partial Differential Equations.* Wiley Interscience.

Matsui, H., Wagner, V., Hill, D., et al. 2006. A physical linkage between cystic fibrosis airway surface dehydration and pseudomonas aeruginosa biofilms. *PNAS* 103, 18131–18136.

Meyer, A., Megerle, J., Kuttler, C., et al. 2012. Dynamics of AHL mediated quorum sensing under flow and non-flow conditions. *Phys. Biol.* 9, 026007.

Müller, J., and Uecker, H. 2012. Approximating the dynamics of communicating cells in a diffusive medium by ODEs – homogenization with localization. *J. Math. Biol.* 53, 0672–702.

Müller, J., Kuttler, C., Hense, B., et al. 2006. Cell-cell communication by quorum sensing and dimension-reduction. *J. Math. Biol.* 53, 0672–702.

Uecker, H., Müller, J., and Hense, B.A. 2014. Individual-based model for quorum sensing with background flow. *Bulletin of Mathematical Biology*, 1–20.

Address correspondence to:
Meltem Gölgeli Matur
Institute of Computational Biology
Helmholtz Zentrum München
Ingolstädter Landstrasse 1
85764 Neuherberg
Germany

E-mail: megolgeli@gmail.com